ELECTROCHEMISTRY IN SILVER CATALYSED FERRIC SULFATE LEACHING OF CHALCOPYRITE

J.D. Miller, P.J. McDonough and H.Q. Portillo

Department of Metallurgy and Metallurgical Engineering
University of Utah

ABSTRACT

Previous investigations have demonstrated the catalytic effect of silver additions in the ferric sulfate leaching of chalcopyrite.

$$CuFeS_2 + 4Fe^{+3} \rightarrow Cu^{++} + 5Fe^{++} + 2S^o$$

The enhanced rate of leaching was found to be due to the formation of an intermediate Ag_2S film which forms on the $CuFeS_2$ surface by an exchange reaction. Under these conditions, unlike the uncatalysed ferric sulfate leach, the elemental sulfur forms a nonprotective reaction product on the Ag_2S crystallites. As a result, the rate appears to become limited by an intermediate electrochemical reaction in the Ag_2S film rather than by transport through the elemental sulfur reaction product.

$$Ag_2S_{(Surface\ CuFeS_2)} + 2Fe^{+3} \rightarrow 2Ag^+ + 2Fe^{++} + S^o$$

The reaction rate was found to have a complex dependence on the Ag^+, Fe^{++} and Fe^{+3} concentrations, but independent of the Cu^{++} concentration. Electrochemical measurements with a Ag_2S-coated chalcopyrite electrode provide furtner information regarding the nature of the reaction mechanism. The kinetics of the rate limiting, intermediate electrochemical reaction are analyzed in terms of the Butler-Volmer equation.

ELECTROCHEMISTRY IN SILVER CATALYSED FERRIC SULFATE LEACHING OF CHALCOPYRITE

J.D. Miller, P.J. McDonough and H.Q. Portillo

Department of Metallurgy and Metallurgical Engineering
University of Utah

Previous investigations have demonstrated the catalytic effect of silver additions in the ferric sulfate leaching of chalcopyrite.

$$CuFeS_2 + 4Fe^{+3} \xrightarrow{Ag^+} Cu^{++} + 5Fe^{++} + 2S^o$$

The enhanced rate of leaching was found to be due to the formation of an intermediate Ag_2S film which forms on the $CuFeS_2$ surface by an exchange reaction. Under these conditions, unlike the uncatalysed ferric sulfate leach, the elemental sulfur forms a nonprotective reaction product on the Ag_2S crystallites. As a result, the rate appears to become limited by an intermediate electrochemical reaction in the Ag_2S film rather than by transport through the elemental sulfur reaction product.

$$Ag_2S_{(Surface\ CuFeS_2)} + 2Fe^{+3} \rightarrow 2Ag^+ + 2Fe^{++} + S^o$$

The reaction rate was found to have a complex dependence on the Ag^+, Fe^{++} and Fe^{+3} concentrations, but independent of the Cu^{++} concentration. Electrochemical measurements with a Ag_2S-coated chalcopyrite electrode provide further information regarding the nature of the reaction mechanism. The kinetics of the rate limiting, intermediate electrochemical reaction are analyzed in terms of the Butler-Volmer equation.

INTRODUCTION

In sulfuric acid solutions of ferric sulfate, chalcopyrite dissolves according to the following reaction,

$$CuFeS_2 + 4Fe^{+3} \rightarrow Cu^{+2} + 5Fe^{++} + 2S^o \qquad (1)$$

This reaction stoichiometry has been observed in a number of investigations. (1-5) Exceptions to this consensus are the early work of Sullivan (6) and the more recent results reported by Jones and Peters. (7) The topochemical nature of the leaching reaction is clearly illustrated in Figure 1 which shows the cross section of partially reacted chalcopyrite particle surrounded by a dense, tenacious sulfur layer.

The formation of an elemental sulfur layer on the chalcopyrite surface may significantly influence the reaction kinetics by establishing a diffusion barrier. The details of rate control for this particular reaction have not been well established. Some investigators (1,7) attribute rate control to a surface reaction. Other investigators (2-5,8,9) report that the reaction rate is limited by transport in the chalcopyrite lattice or through the elemental sulfur reaction product layer. Differences in leaching behavior reported in the literature (5) may be due to variations in the intrinsic electrochemical properties

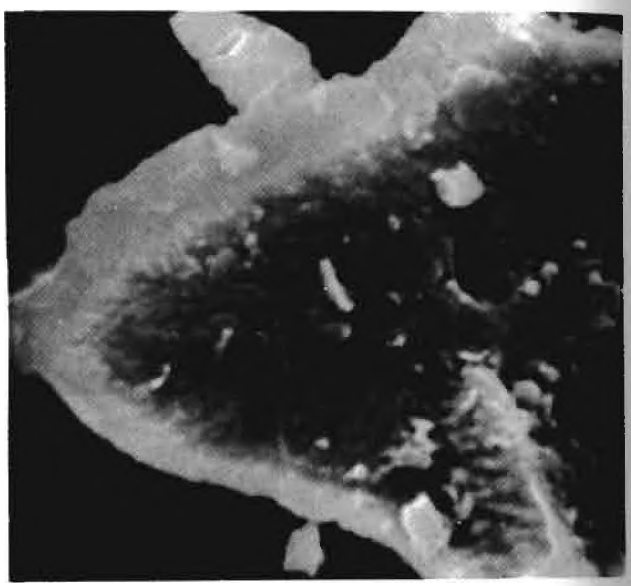

Figure 1. SEM photograph of the cross section of a partially leached chalcopyrite particle (10 μm) showing the sulfur layer and topochemical nature of the uncatalysed ferric sulfate leach. (5)

of the chalcopyrites used in the various studies. These electrochemical differences are illustrated by the anodic polarization curves presented in Figure 2. (10)

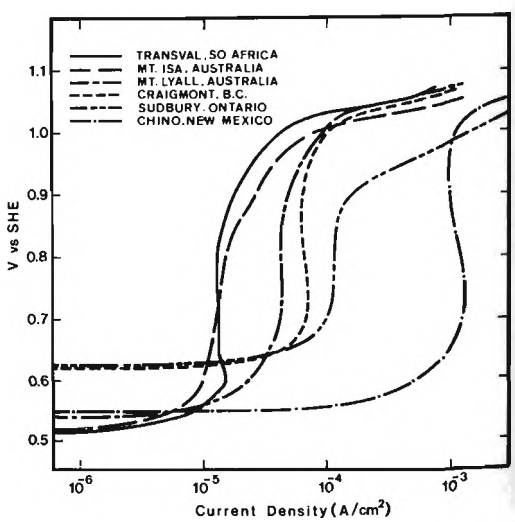

Figure 2. Anodic polarization curves for $CuFeS_2$ from six different locations in 1 M H_2SO_4, 30 mv/min, 25°C. (10)

Notice that the current density for a fixed potential can differ by as much as two orders of magnitude for different samples of chalcopyrite.

Most recently, leaching data for passive chalcopyrites which exhibit parabolic reaction kinetics have been reconsidered together with new experimental data and the results interpreted using Wagner's theory of oxidation. (5) Analysis of the ferric sulfate leaching system in this context suggests that the rate limiting process may be the transport of electrons through the elemental sulfur layer as depicted schematically in Figure 3.

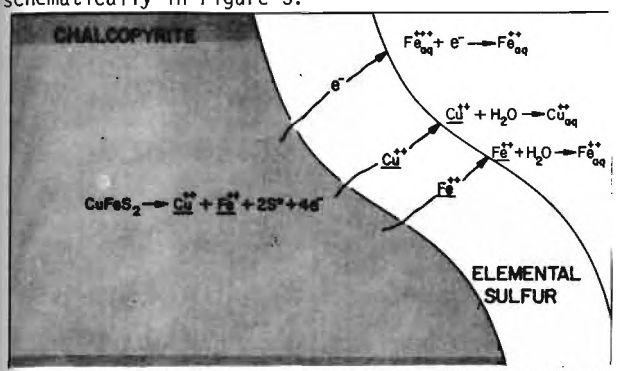

Figure 3. Schematic representation of the transport process in the ferric sulfate leaching of chalcopyrite. Note that the hydrated ferric ion does not advance through the sulfur product layer, but rather is discharged at the sulfur-solution interface. The analysis does not distinguish Cu^{++} and Fe^{+++} from Cu^{+} and Fe^{++} as the transported species. (5)

Predicted reaction rates calculated from first principles using the physicochemical properties of the system (conductivity of elemental sulfur, t σ, and the free energy change for the reaction, $\Delta G°$) agree satisfactorily with experimentally determined rates. This analysis is summarised in Table I.

Table I. Ferric Sulfate Leaching of Chalcopyrite in the Absence of Silver (5)

The rate of acid ferric sulfate leaching of monosize chalcopyrite particles in a stirred reactor appears to be limited mainly by the transport of electrons through the elemental sulfur reaction product. This position has been analysed in terms of Wagner's theory of oxidation and is supported by:

1) Independence of rate on both reactant and product concentrations.
2) Parabolic reaction kinetics.
3) A rate constant equivalent in magnitude (7.6×10^{-13} ohm^{-1}cm^{-1}) to the electrical conductivity of elemental sulfur (10^{-13} ohm^{-1}cm^{-1}).
4) An apparent activation energy, 20 kcal/mole (83.7 kJ/mole) equivalent to the temperature coefficient for electrical conduction in elemental sulfur, 23 kcal/mole (96.2 kJ/mole).

Silver Catalysis

It has been demonstrated that silver addition in acid ferric sulfate leaching of chalcopyrite and similar systems (11-13) accelerates greatly the rate

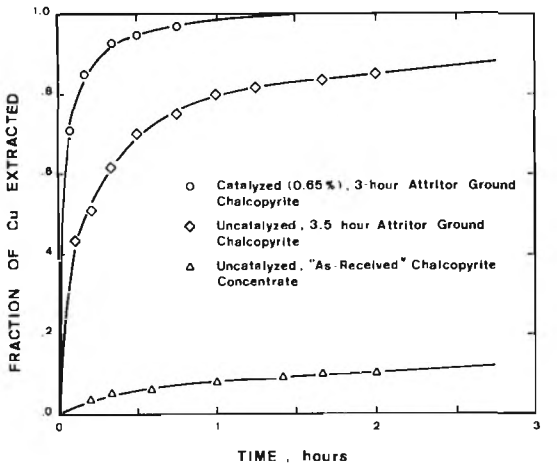

Figure 4. Fraction of copper extraction as a function of time for different products at 1 M Fe^{+3} and 90°C. (14)

of reaction. For example, the catalysed and uncatalysed leaching rates for an attritor-ground chalcopyrite are contrasted in Figure 4. (14)

Some mechanistic information on this catalytic effect has been reported. However, further research is required to elucidate details of the intrinsic reaction kinetics.

Silver Exchange Reaction

The reaction of silver ion with chalcopyrite in the absence of oxidant has been found to be described by the following exchange reaction (14)

$$CuFeS_2 + 4Ag^+ \rightarrow 2Ag_2S_{(Surface)} + Cu^{++} + Fe^{++} \quad (2)$$

Chalcopyrite when reacted with silver ion rapidly forms a blue-black product on the chalcopyrite surface. Analysis on this reaction product by x-ray diffraction showed that the reaction product consisted of Ag_2S (argentite) and unreacted $CuFeS_2$ with all reported "d" spacings identified. Solution analyses, however, showed some deviation from the indicated stoichiometry. The results obtained seem to be independent of acid strength (0.1 M to 1.0 M H_2SO_4) at 90°C.

The initial kinetics of the exchange were determined by following the depletion of silver ion with a specific ion electrode and were studied as a function of initial silver concentration, particle size, and temperature. (14) Generally the initial kinetics were first order with respect to silver concentration until the thickness of the Ag_2S film exceeded approximately 50A°. For the case of first order reaction kinetics, the reaction velocity constant can be found from a semi-log plot and should be independent of the initial silver concentration. Such was found to be the case for a wide range of concentrations (over 2 orders of magnitude) and for two different monosize samples (4.8 μm and 51.2 μm) at 25° as shown in Figure 5.

The effect of particle size was also considered in the analysis of the initial reaction kinetics. Gener-

ally the reaction velocity constant would be expected to be largely independent of the particle size even for rate control by diffusion in the mass transfer boundary layer. It was found that the reaction velocity constants for the 4.8 μm and 51.2 μm samples do not differ greatly, 2.67×10^{-2} cm/sec and 1.28×10^{-2} cm/sec respectively. The initial high rate of this first order reaction would suggest that the rate may be limited by diffusion in the mass transfer boundary layer. To test this hypothesis, the experimental reaction velocity constants were compared to predicted mass transfer coefficients for stirred reactors estimated using Harriot's approach (15,16) which is based on the Sherwood correlation. (17) Excellent agreement between experimental and predicted values was obtained.

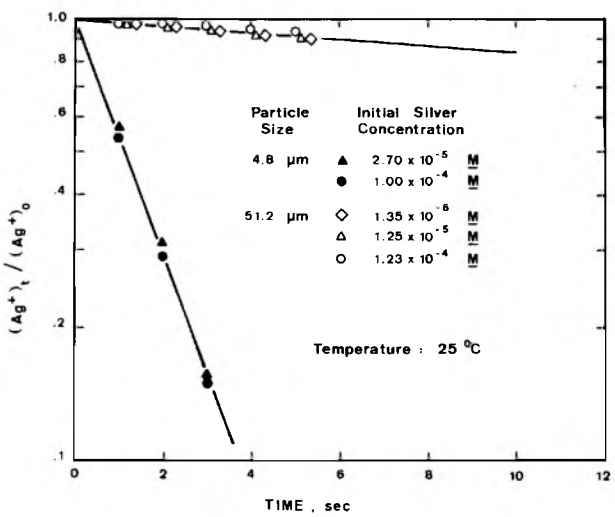

Figure 5. First order rate plot of fraction of silver reacted for two monosize chalcopyrite samples at 0.25 M H_2SO_4, 0.2 percent solids, 600 rpm and various initial silver concentrations. (14)

Finally, if the initial reaction kinetics are controlled by a mass transfer process in the aqueous phase, then the temperature coefficient for the rate phenomenon should typically correspond to an activation energy of less than 5.0 kcal/mole (20.9 kJ/mole). An apparent activation energy of 4.2 kcal/mole (17.6 kJ/mole) was found for the 51.2 μm material which supports the hypothesis of rate control by mass transfer in the aqueous phase. Similar results were obtained for the 4.8 μm sample with an apparent activation energy of 3.1 kcal/mole (13.0 kJ/mole).

Silver Catalysed Ferric Sulfate Leach

The silver catalysed reaction appears to exhibit the same stoichiometry as the uncatalysed reaction presented in Equation 1. (14) In the absence of the chloride salts, elemental sulfur together with Ag_2S constituted the reaction product as determined by x-ray diffraction. Solution analyses for copper and ferrous revealed a Fe^{++}/Cu^{++} mole ratio of 5.08 (average of 18 values from 4 different experiments) at all stages of the reaction which closely corresponds to the 5/1 ratio specified by the stoichiometry of the suggested reaction in Equation 1.

The leaching response was found to be sensitive to the experimental procedure used for reaction initiation. As might be expected when the chalcopyrite was allowed to react first with the ferric sulfate the reaction kinetics were slow due to the formation of the impervious elemental sulfur layer during the initial time interval prior to the addition of silver. On the other hand, when the silver was added first a much more rapid leaching response was observed.

Further, the rate and extent of reaction were found to be dependent on the initial silver concentration. The rate increased with an increase in initial silver concentration up to 1×10^{-3} M. Further additions beyond this level did not enhance the rate of reaction and even reduced the rate significantly.

Particle Size. One of the most diagnostic features in the analysis of kinetic data is the particle size dependence of the reaction rate. An inverse first order dependence on the initial particle size could be indicative of rate control by diffusion in the aqueous phase or by surface reaction. An inverse second order dependence on the initial particle size would suggest rate control by diffusion through a growning reaction product layer. Neither case was observed in the silver catalysed ferric sulfate leaching of chalcopyrite. Surprisingly, the rate, up to approximately 50% reacted, was essentially independent of initial particle size as shown in Figure 6.

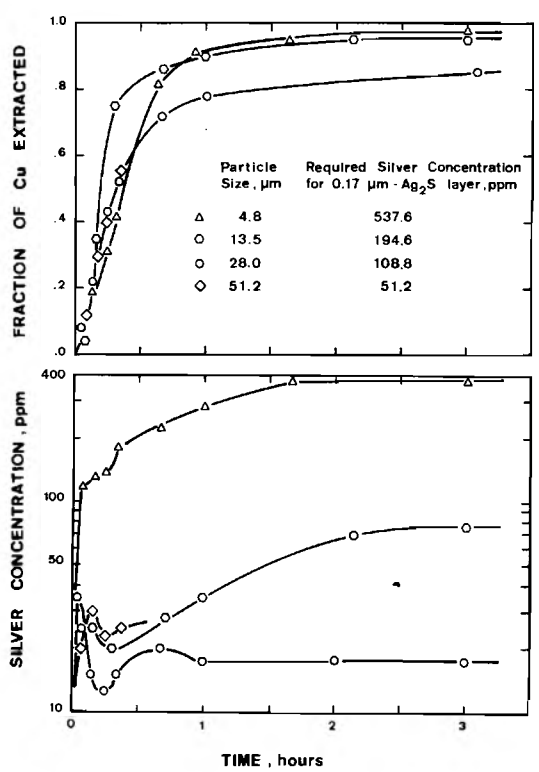

Figure 6. The effect of particle size on the rate and extent of the catalysed reaction at 0.25 M H_2SO_4 1.0 M Fe^{+3}, 0.3 percent solids, 600 rpm and 90°C. Also the corresponding plot of silver concentration in the aqueous phase as a function of reaction time is shown for the respective experiments.

These experiments were done by first completing the exchange reaction and establishing a silver sulfide layer of fixed thickness (0.174 μm) assuming spherical particles of a specified median particle size.

It is clear from the data that the Ag_2S film reacts rapidly with the ferric sulfate solution as revealed by the plots of silver concentration in the aqueous phase as a function of time.

$$Ag_2S_{(Surface)} + 2Fe^{+3} \rightarrow 2Ag^{+} + 2Fe^{2+} + S^{o} \quad (3)$$

The silver sulfide layer is not completely removed and a rapid rate of chalcopyrite leaching, independent of initial particle size was observed. Under certain circumstances for the 51.2 μm sample the Ag_2S film dissolved completely during the first few minutes and the reaction became passivated due to sulfur formation at the chalcopyrite surface.

Only after extensive reaction ($\gtrsim$ 50% reacted), does the sulfur layer, which appears to form in the silver film, become protective. The very distinct difference between the sulfur which forms in the silver catalysed reaction and that which forms during the uncatalysed reaction is revealed by the SEM photographs presented in Figure 7. Note that the surface sulfur created in the case of the silver catalysed reaction is very porous with well defined sulfur crystallites seen. In the case of the uncatalysed reaction a smooth tenacious layer of elemental sulfur forms similar to that shown in cross section in Figure 1.

Concentration Effects. Unlike the uncatalysed reaction, a definite Fe^{+3} dependence of the rate was observed in the case of the silver catalysed reaction. In addition, the reaction kinetics were extremely sensitive to the Fe^{+2} concentration as shown in Figure 8. Note that the addition of 0.5 M $FeSO_4$ essentially passivates the system and very little reaction is achieved. On the other hand, the addition of 0.5 M $CuSO_4$ or $MgSO_4$ does not alter the reaction rate. These results are somewhat anomalous in that the rate is dependent on the concentration of one of the reaction products (Fe^{++}) but independent of the concentration of another reaction product (Cu^{++}).

On the basis of these observed results it was suggested (14) that the rate may be controlled by the intermediate electrochemical reaction of Ag_2S with Fe^{+3}.

$$Ag_2S_{(Surface)} + 2Fe^{+3} \rightarrow 2Ag^{+} + 2Fe^{++} + S^{o} \quad (3)$$

It was hypothesized that this electrochemical reaction occurs at the surface of silver sulfide crystallites throughout the Ag_2S film. The crystallites act as short circuited microelectrodes allowing for the discharge of Fe^{+3} and the release of Ag^{+}. Under these circumstances, the kinetics could show a dependence on the Ag^{+}, Fe^{+3}, and Fe^{++} concentrations and would be independent of the initial particle size, i.e. the rate is dependent on the internal area of the crystallites rather than on the external area of the particle. It was suggested that elemental sulfur replaces the Ag_2S crystallites forming a porous, non-protective layer. The silver ion generated acts as a transfer agent while the silver sulfide film, necessary to prevent extensive sulfur formation at the chalcopyrite surface, is continually restored. A schematic representation of this mechanism is presented in Figure 9.

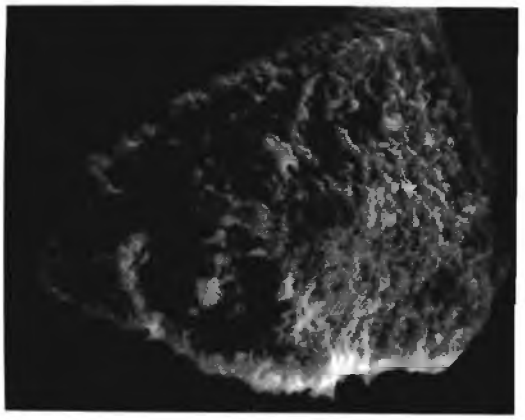

Partially Reacted 28 μm Particle -- Catalized

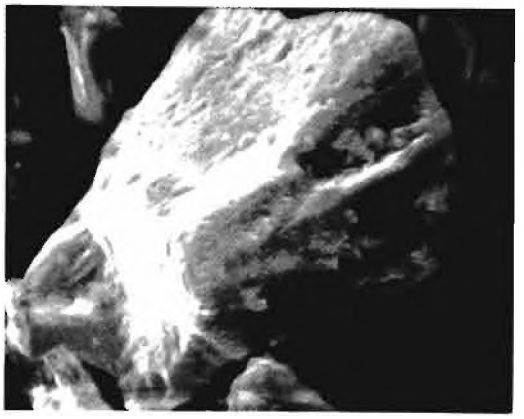

Partially Reacted 28 μm Particle -- Uncatalized

Figure 7. SEM photographs contrasting the nature of the elemental sulfur reaction product layer which forms during the catalysed reaction with that which forms during the uncatalysed reaction.

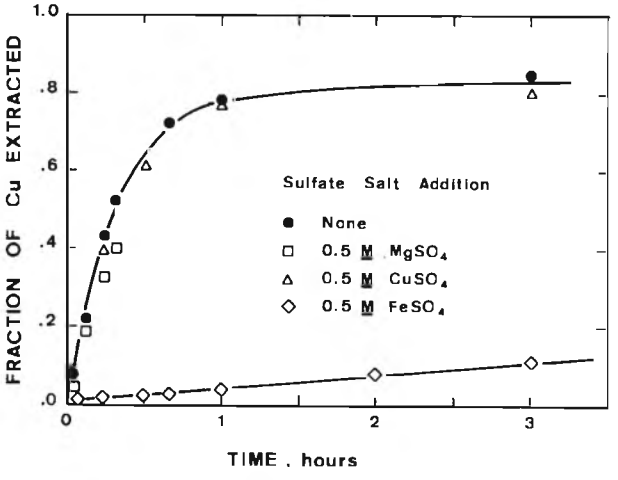

Figure 8. The effect of ferrous sulfate addition on the rate and extent of reaction for 28 μm particles at 0.25 M H_2SO_4, 1 M Fe^{+3}, 0.3 percent solids, 600 rpm and 90°C. (0.17 μm Ag_2S layer). (14)

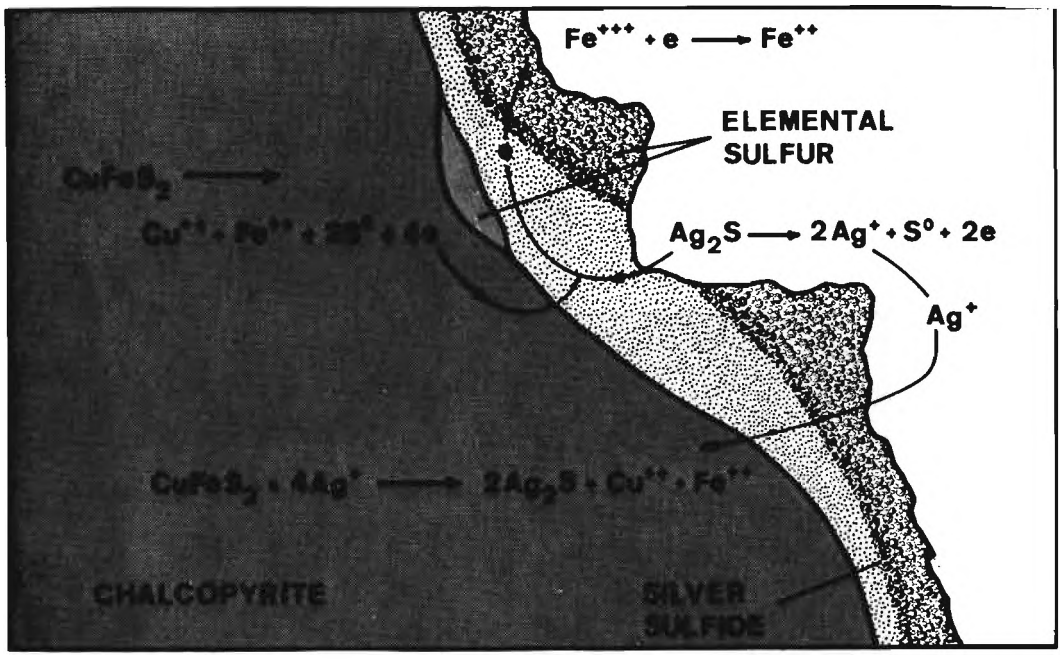

Figure 9. Schematic representation of the silver catalyzed ferric sulfate leaching of chalcopyrite with possible reactions of kinetic importance included.

EXPERIMENTAL TECHNIQUES

Two types of experiments were done in this study; leaching experiments in a stirred reactor and rest potentials measurements for a chalcopyrite electrode using a nulling circuit with a high impedance voltameter.

Materials

The chemicals used in this investigation were of reagent grade quality and the water used was distilled and deionized. For the silver catalysed ferric sulfate leaching experiments, monosize particles from a Pima flotation concentrate were prepared by wet screening and sizing with a Warman Cyclosizer. Elimination of particle aggregates was accomplished by dispersion with an ultrasonic probe. Gangue particles, primarily quartz, silicates and pyrite were removed by magnetic separation. The prepared samples were found to have the properties reported in Table II. (14,15)

Table II. Physical and Chemical Properties of Monosize Chalcopyrite Samples

Median Size (microns)	Chemical Analysis % Cu	% Fe	Specific Surface Area (m^2/gr)	Specific Gravity
4.8	26.5	29.5	0.480	3.75
13.5	30.5	28.5	0.195	3.92
28.0	31.5	30.5	0.092	3.92
51.2	33.5	30.5	0.031	3.92

The chalcopyrite sample used for rest potential measurements was from Transvaal, South Africa. The massive specimen is reported to be void of other sulfide phases such as cubanite ($CuFe_2S_3$) and pyrrhotite (FeS) both from mineralogical analysis and by x-ray analysis. (10) The sample of Transvaal Chalcopyrite was found to contain only minor amounts of quartz. A portion of this sample was cut into a rectangular parallelepiped the dimensions of which were 1 cm x 1 cm x 0.1 cm. One side of this parallelepiped was sputtered with a gold film to provide for low ohmic resistance and the sample was mounted in thermal plastic with provision for electrical contact via a mercury and platinum wire junction. The chemical reacting surface was polished with 1 μm diamond paste to clean the surface and establish a known area for subsequent current density determinations.

Leaching Experiments

Leaching experiments were carried-out under an atmospheric pressure of nitrogen using a four-necked unbaffled cylindrical reactor submerged in a constant temperature oil bath. The stirring speed was kept constant at 600 rpm, controlled with a Dyna-Mix variable speed stirrer. All experiments were carried-out in a total volume of 1 liter. Temperature of the bath was maintained within ±0.2°C. An initial two-hour acid wash (0.25 M H_2SO_4) of the monosize samples was necessary to remove and correct the kinetic data for acid soluble copper.

The following procedure was used to follow the silver catalysed acid ferric sulfate leaching of chalcopyrite.

1) A specified amount of ferric sulfate was dissolved with a minimum of the 0.25 M sulfuric acid solution. The ferric solution was heated separately to the desired temperature before pouring into the reactor.

2) The reactor was filled with the remaining amount of 0.25 M sulfuric acid solution and heated to the desired temperature at which time the monosize sample was introduced into the reactor.

3) After two hours of washing a 3 cc sample was withdrawn just before introducing the silver solution (~2 cc) necessary to achieve the desired silver concentration.

4) After the addition of the silver solution (30 sec), the ferric solution (prepared in step 1) was poured into the reactor. This was the starting point (time zero) for determination of the rate of reaction.

It should be pointed out that the sequence; solids, silver solution, and ferric solution was selected because it gave the most rapid kinetic response. All samples (3 cc) taken at timed intervals were cooled immediately in a container of ice. After cooling, the samples were centrifuged and the aqueous phase diluted as necessary and analysed for copper and/or ferrous concentrations. The extent of reaction was calculated in terms of the fraction of the copper extracted from the acid-washed sample.

Rest Potential Measurements

The rest potential measurements were made in a typical electrochemical cell (Figure 10) where the calomel reference electrode was separated by a Luggin capillary filled with Na_2SO_4 solution and the platinum button counter electrode was separated from the working Ag_2S-coated chalcopyrite electrode by a fritted glass membrane. The Ag_2S-coated electrode was prepared by reacting the chalcopyrite surface with a sulfuric acid silver nitrate solution. Based on depletion of the Ag^+ from solution a thickness of Ag_2S was calculated to be 6.8×10^{-6} cm. The electrochemical cell was purged with argon and submerged in the constant temperature oil bath mentioned previously.

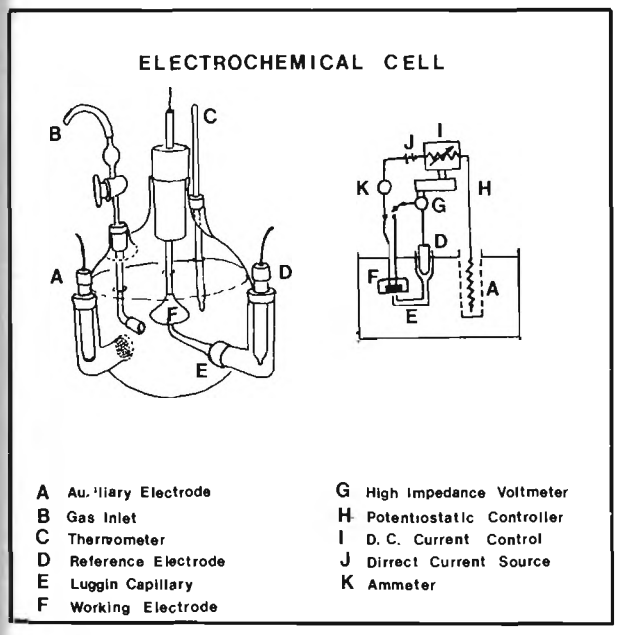

Figure 10. Schematic diagram of the electrochemical cell used for the rest potential measurements of silver coated chalcopyrite.

The electrode was rotated and controlled by a Dyna-Mix variable speed stirrer. The rest potentials were measured using a Princeton Applied Research Model 173 potentiostat and a Model 175 potential sweep generator.

EXPERIMENTAL RESULTS AND DISCUSSION

New rate data for the silver catalysed ferric sulfate leach of chalcopyrite is reported and analysed together with rest potential measurements in terms of an electrochemical reaction mechanism.

Leaching Experiments

In addition to previous experimental results (14) summarized in the introduction, other more recent experiments have further revealed the nature of the silver catalysed ferric sulfate leach. Rate data is presented as a function of concentration variations and as a function of temperature.

Concentration Effects

Unlike the uncatalysed ferric sulfate leach, (5) a significant dependence on ferric sulfate addition was observed for the silver catalysed system. This effect was not studied extensively. However, a reaction order of approximately 0.5 was estimated with respect to ferric ion. Anomalous results were observed at higher ferric concentrations (>1 M Fe^{+3}) which may involve transport problems or solution chemistry complications. Figure 11 shows the extraction of copper as function of time with ferric ion concentration as the parameter. Note that under these circumstances of higher silver addition, 4×10^{-3} M, the linear reaction kinetics observed previously (see Figure 6) do not prevail. These nonlinear results, besides demonstrating the ferric ion dependence, may

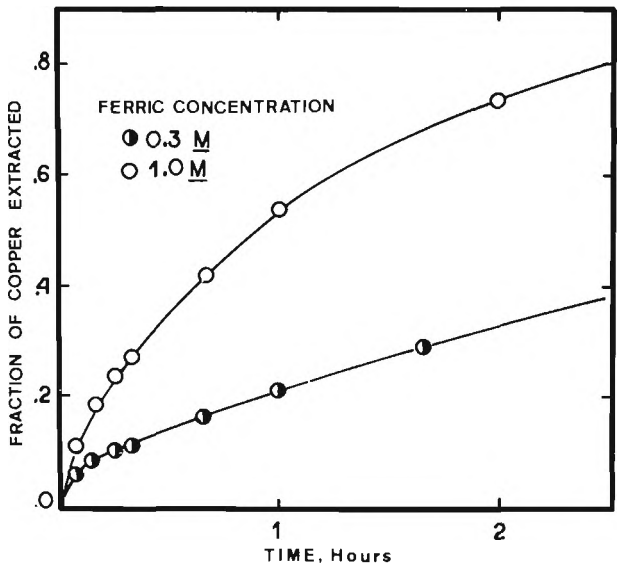

Figure 11. Influence of the initial ferric concentration on the extent of the catalysed reaction for 28 μm particles at 0.25 M H_2SO_4, 4×10^{-3} M Ag^+, 0.3 percent solids, 600 rpm and 90°C.

also reflect a reaction resistance due to transport through the reacting silver sulfide film which would be expected for a thicker layer of silver sulfide. However, the initial reaction kinetics for 1 M $Fe_2(SO_4)_3$ (open circles) are about the same as those observed for lower levels of silver addition, 10^{-3}M at 1 M $Fe_2(SO_4)_3$ (open circles) presented in Figure 6. The departure from linearity at the higher silver concentration and the slower rate of reaction also suggests that Ag^+ may inhibit the reaction via back reaction kinetics just as had been observed in the case of Fe^{++}. Recall that an addition of 0.5 M $FeSO_4$ essentially passivates the system and very little reaction is achieved as was shown in Figure 8. To test further the notion that the Ag^+ concentration can diminish the reaction rate, diagnostic experiments were attempted; the results of which are shown in Figure 12. Again, it can be noted that the initial rate is essentially independent of the amount of silver sulfide formed but for higher levels of silver addition (more silver sulfide on the surface initially), the rate decreases during intermediate reaction times (10 min. to 60 min.). Furthermore, the subsequent injection of silver (300 ppm) into the system after the catalysed ferric sulfate reaction had been initiated at 108 ppm silver (closed circles) reduces the rate considerably.

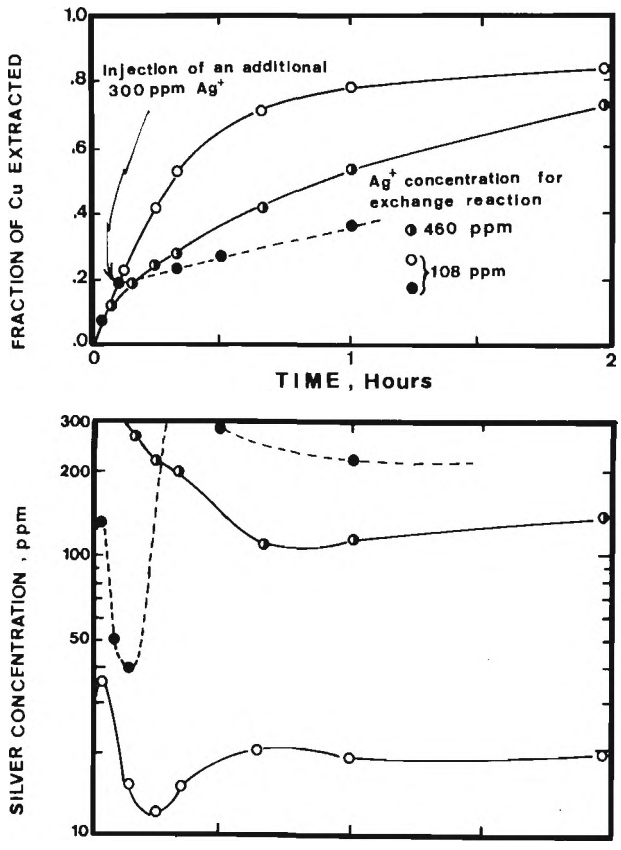

Figure 12. The effect of silver concentration on the rate and extent of reaction for 28 μm particles at 0.25 M H_2SO_4, 1 M Fe^{+3}, 0.3 percent solids, 600 rpm and 90°C.

Temperature

A significant temperature dependence on the reaction rate is observed for the catalysed ferric sulfate leach of the 4.8 μm sample as shown in Figure 13. In this particular set of data the ferric concentration is of sufficient excess so as to be considered constant which facilitates analysis of the experimental data. In addition, it is very important, as discussed earlier, to evaluate the temperature effect at constant, steady-state silver concentration (∿25 ppm in aqueous phase). An Arrhenius plot of the data is presented in Figure 14 and an apparent activation energy of 15.7 kcal/mole (65.7 kJ/mole) is observed for this rate process.

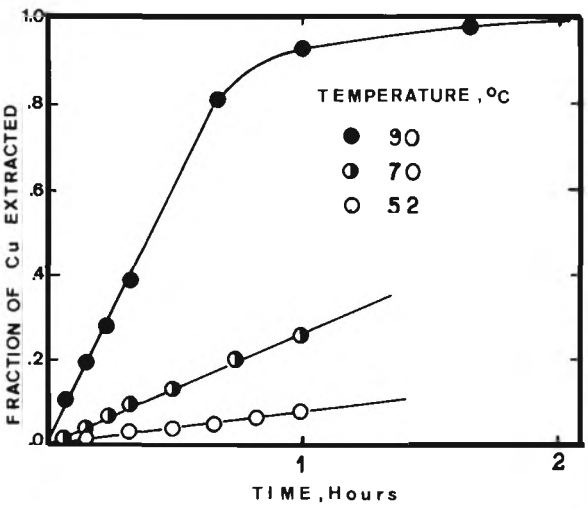

Figure 13. The influence of temperature on the rate and extent of the catalyzed reaction for 4.8 μm particles at 0.25 M H_2SO_4, 1 M Fe^{+3}, 0.3 percent solids and 600 rpm. (0.17 μm Ag_2S layer).

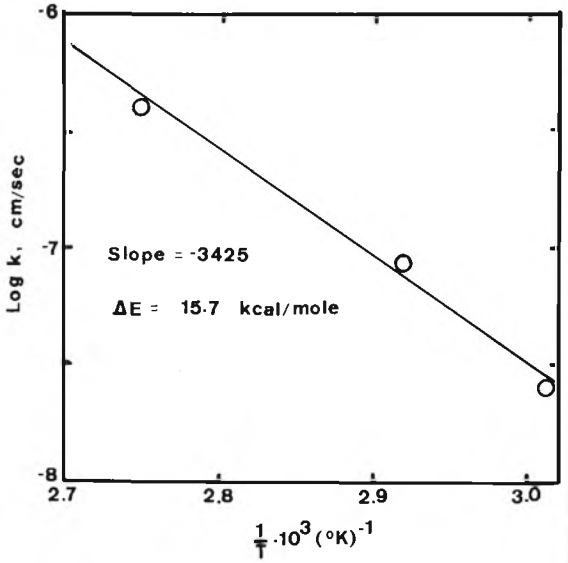

Figure 14. Arrhenius plot of the reaction velocity constant for the silver catalysed leaching of chalcopyrite with the 4.8 μm monosize chalcopyrite sample after having formed 0.17 μm layer of Ag_2S. Data taken from Figure 13.

The experimental reaction velocity constants used in construction of the Arrhenius plot were calculated assuming a first order rate process with respect to the reactant concentration, the Fe^{+3} concentration.

Values for the reaction velocity constant are on the order of 2.21×10^{-8} to 3.48×10^{-7} cm/sec, orders of magnitude less than the appropriate mass transfer coefficients ($\sim 10^{-2}$ cm/sec) which would be predicted if the rate were limited by diffusion in the mass transfer boundary layer.

These results together with those results published earlier (14) and summarized in the introduction (p.12) seem to sustain the original hypothesis that the silver catalysed reaction of chalcopyrite with ferric sulfate is limited by intermediate electrochemical reaction,

$$Ag_2S_{(Surface)} + 2Fe^{+3} \rightarrow 2Ag^{+} + 2Fe^{++} + S^{o} \qquad (3)$$

Electrochemistry

The electrochemistry of the silver catalysed ferric sulfate leaching of chalcopyrite reaction is examined in terms of rest potential measurements used to explain the leaching kinetics in the context of the Butler-Volmer equation.

Rest Potential Measurements

The rest potential of the Ag_2S-coated chalcopyrite electrode was measured as a function of Ag^{+} concentration at 80°C. The linear relationship presented in Figure 15 shows that the electrode exhibits Nernstian behavior with an estimated standard potential of 787 mv and a slope of 69.8 mv per decade of concentration change. These results suggest that the electrode may be measuring the following half cell reaction,

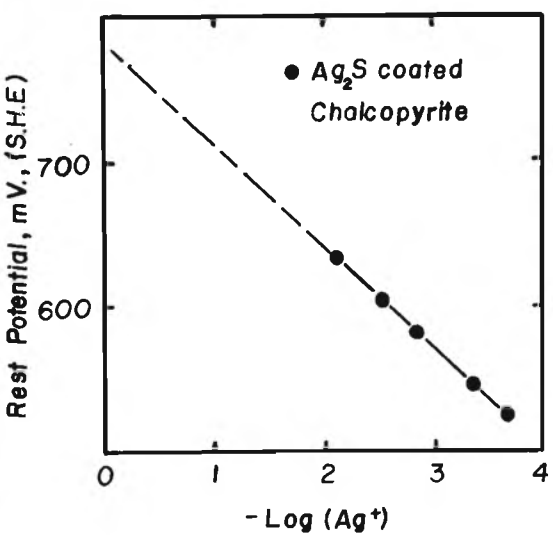

Figure 15. Rest potential of Ag_2S-coated chalcopyrite as a function of Ag^{+} concentration at 0.25 M H_2SO_4 and 80°C.

$$Ag_2S \rightleftarrows 2Ag^{+} + S^{o} + 2e \qquad (4)$$

the standard potential for which is reported to vary from 799 mv to 1000 mv at 25°C. At higher temperatures lower rest potentials would be expected due to a negative temperature coefficient. (18) Similarly, the observed slope is close to that predicted at 80°C from the Nernst equation, 70.1 mv per decade change in concentration.

Other results shown in Figure 16 support this hypothesis inasmuch as the potential of the Ag_2S-coated chalcopyrite electrode is insensitive to Fe^{++} additions; whereas the potential of the uncoated chalcopyrite electrode exhibits a very definite dependence on the Fe^{++} addition. These results suggest that the Ag_2S film completely seals the chalcopyrite surface and a Nernstian half cell potential for Ag_2S is measured rather than a mixed potential involving a chalcopyrite half cell reaction.

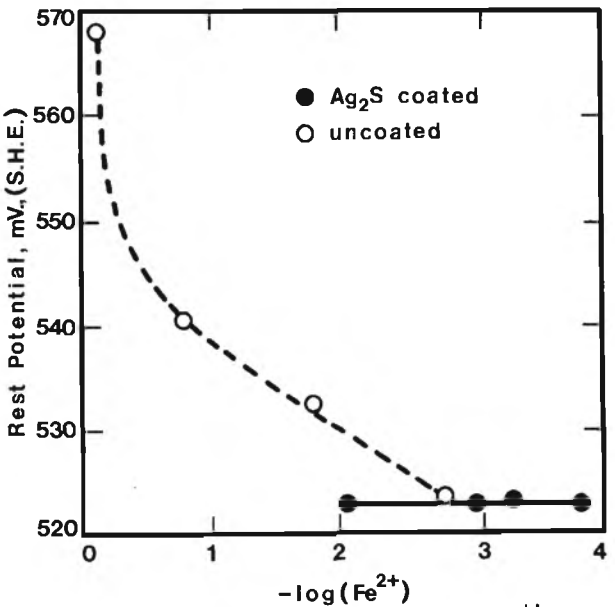

Figure 16. Rest potential as a function of Fe^{++} concentration at 0.25 M H_2SO_4 and 80°C.

Reaction Mechanism

The key to understanding the rate enhancement which occurs during silver catalysis in ferric sulfate leaching of chalcopyrite is the very dramatic change in the nature of the sulfur deposit as shown by the photographs presented in Figure 7. The sulfur layer no longer inhibits the reaction progress as it does in the uncatalysed ferric sulfate leach. This observation together with the following data suggest that the leaching rate is controlled by the rate of an intermediate electrochemical reaction in the Ag_2S film;

$$Ag_2S + 2Fe^{+3} \rightarrow 2Ag^{+} + 2Fe^{++} + S^{o} \qquad (3)$$

1) magnitude of reaction velocity approximately 10^{-8} cm/sec, orders of magnitude less than predicted mass transfer coefficients (10^{-2} cm/sec)
2) independence of reaction rate on particle size
3) complex dependence of reaction rate on Ag^{+}, Fe^{+3}

and Fe^{++} concentrations and independence of reaction rate on Cu^{++} concentration.
4) Apparent activation energy 15.7 kcal/mole (65.7 kJ/mole).

Thermodynamics. The standard free energy change for this particular reaction (Equation 3) at 90°C is $\Delta G^{\circ}_{90°C} \simeq 5.0$ kcal/mole which was determined by interpolation since no thermodynamic data was available at this particular temperature. (19,20) A plot of the standard free energy of reaction vs. temperature is presented in Figure 17.

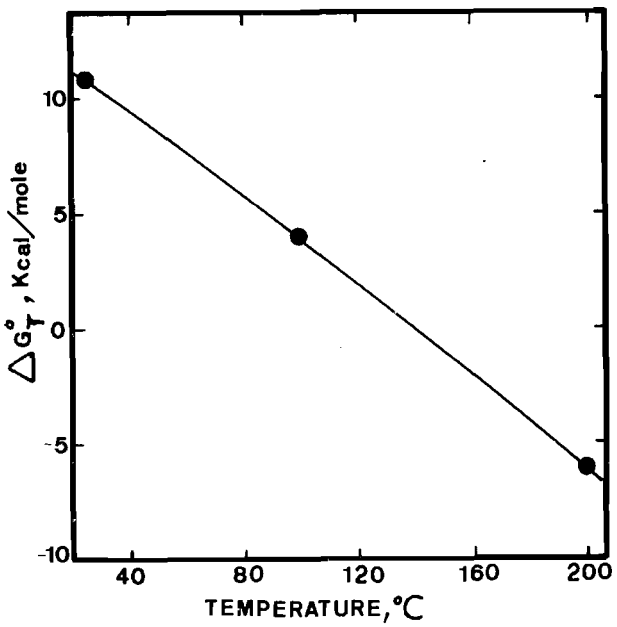

Figure 17. Standard free energy change as a function of temperature for the intermediate electrochemical reaction.

As can be seen under experimental conditions the reaction is close to equilibrium and as a result will be quite sensitive to slight changes in temperature and the composition of the aqueous phase. Complete evaluation of the possibility of rate control by this intermediate electrochemical reaction requires further thermodynamic analysis. In particular, the activities of the various species must be specified and the free energy of reaction determined at the temperatures of interest. By this approach conditions under which the intermediate reaction is thermodynamically feasible can be identified. The results of this thermodynamic analysis are presented in Figure 18. The set of surfaces for different temperatures specify the thermodynamic stability for various solution compositions.

Compositions which lie above a given surface correspond to conditions under which the intermediate electrochemical reaction should not occur. Whether or not the reaction should occur under specified temperature and aqueous phase composition can be determined if the activities of the reactants and products are known. These values can be determined using the University of Utah Solution Chemistry Program. For example, let's examine the experiment involving 0.5 M $FeSO_4$ which was presented in Figure 8. Computer analysis of the solution chemistry of this system results in the following activities:

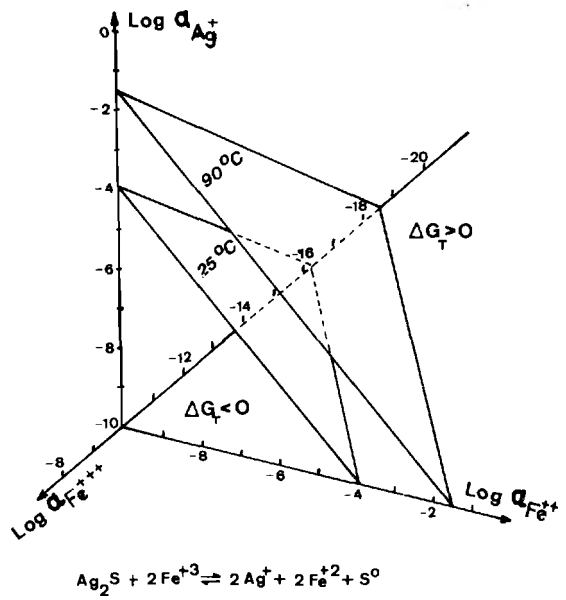

Figure 18. Equilibrium surfaces of the intermediate electrochemical reaction as a function of solution composition at 25°C and 90°C.

$$a_{Fe^{+3}} = 1.1 \times 10^{-3}$$
$$a_{Fe^{+2}} = 3.55 \times 10^{-2}$$
$$a_{Ag^+} \simeq 4.64 \times 10^{-4}$$

Evaluation of the free energy of reaction for these activities results in a value of -0.9 kcal/mole which indicates that the reaction should occur, but as can be seen in Figure 8 the reaction is exceedingly slow.

The independence of the rate on initial particle diameter suggests that the reaction kinetics are controlled by electrochemical discharge at the surface of the individual Ag_2S crystallites as shown by the schematic representation of the reaction mechanism in Figure 9. The crystallites act as short circuited microelectrodes allowing for the discharge of Fe^{+3} and the release of Ag^+. Under these circumstances the kinetics could show a dependence on the Fe^{+3}, Fe^{+2} and Ag^+ concentrations and would be independent of the initial particle size, i.e. the rate is dependent on the internal area of the crystallites rather than on the external area of the particle. In addition the strong sensitivity of the leaching rate to the Fe^{++} concentration suggests that either the back reaction kinetics are important or that the dependence arises from a mixed potential developed in the Ag_2S film during reaction. SEM photographs indicate that elemental sulfur replaces the Ag_2S crystallites forming a porous nonprotective layer.[2] The silver ions generated act as a transfer agent while the silver sulfide film, necessary to prevent extensive sulfur formation at the chalcopyrite surface, is continually restored in the exchange reaction.

The highly irreversible exchange reaction would not be rate limiting due to the rate dependence on ferric ion concentrations and the rate independence on the cupric ion concentration. Eventually, after ~50%

reaction, the rate becomes nonlinear (see Figure 6) and apparently enough sulfur forms to provide significant resistance to mass transport.

Butler-Volmer Equation. If the intermediate electrochemical reaction (Equation 3) is considered in terms of its respective half cell reactions:

anodic half cell,

$$Ag_2S \rightarrow 2Ag^+ + S^0 + 2e^- \qquad (4)$$

cathodic half cell,

$$Fe^{++} \rightarrow Fe^{+3} + e \qquad (5)$$

which occur at distinct anodic and cathodic sites and are short-circuited through the Ag_2S film, then the reaction kinetics can be evaluated in terms of the Butler-Volmer equation. (18) If ohmic potentials are small then the system developes a mixed potential (E_m), a compromise potential, under which conditions the anodic current (i_a) equals the cathodic current (i_c). Assuming a first order dependence on reacting species as well as single electron transfer processes and transfer coefficients equal to 0.5, the partial currents for the respective half cells would be;

$$i_a = A_a z_a F \vec{k}_a \exp\left(\frac{FE_m}{2RT}\right) - A_a z_a F (Ag^+) \overleftarrow{k}_a \exp\left(-\frac{FE_m}{2RT}\right) \qquad (6)$$

and

$$i_c = A_c z_c F (Fe^{++}) \vec{k}_c \exp\left(\frac{FE_m}{2RT}\right) - A_c z_c F (Fe^{+3}) \overleftarrow{k}_c \exp\left(-\frac{FE_m}{2RT}\right) \qquad (7)$$

Since these half cell reactions have been assumed to be short-circuited,

$$i_a = - i_c \qquad (8)$$

it follows that

$$\exp\left(\frac{FE_m}{RT}\right) = \frac{A_c z_c (Fe^{+3}) \overleftarrow{k}_c + A_a z_a (Ag^+) \overleftarrow{k}_a}{A_c z_c (Fe^{++}) \vec{k}_c + A_a z_a \vec{k}_a} \qquad (9)$$

The reaction rate can then be formulated from the expression for either partial current in terms of the mixed potential as well as reactant and product concentrations,

$$-\frac{dn}{dt} = \frac{i_a}{z_a F} = A_a \vec{k}_a \left[\frac{A_c z_c (Fe^{+3}) \overleftarrow{k}_c + A_a z_a (Ag^+) \overleftarrow{k}_a}{A_c z_c (Fe^{++}) \vec{k}_c + A_a z_a \vec{k}_a}\right]^{1/2} - A_a (Ag^+) \overleftarrow{k}_a \left[\frac{A_c z_c (Fe^{++}) \vec{k}_c + A_a z_a \vec{k}_a}{A_c z_c (Fe^{+3}) \overleftarrow{k}_c + A_a z_a (Ag^+) \overleftarrow{k}_a}\right]^{1/2} \qquad (10)$$

Apparent reaction orders are difficult to determine from such an expression which includes consideration of back reaction kinetics, which is reasonable in terms of the thermodynamic analysis presented previously. This complexity together with possible variation of anodic and cathodic areas during the course of the reaction makes it difficult to simplify the kinetic expression. However, it should be evident that, generally, increased Fe^{+++} concentration should enhance the rate of reaction, whereas increased Fe^{++} and Ag^+ concentrations should reduce the rate.

Evaluation of the Butler-Volmer equation for conditions under which back reaction kinetics are not significant, simplifies the rate expression to a certain extent;

$$-\frac{dn}{dt} = \frac{i_a}{z_a F} = A_a \vec{k}_a \frac{A_c z_c (Fe^{+3}) \overleftarrow{k}_c}{A_a z_a \overleftarrow{k}_a} \qquad (11)$$

in which case it is seen that the rate is independent of Fe^{++} and Ag^+ concentrations and has a one half order dependence on the Fe^{+3} concentration. In view of the experimental results, such a condition might only prevail for initial reaction kinetics and the limited data presented in Figure 11 would tend to support this premise.

SUMMARY AND CONCLUSIONS

Silver catalysis in acid ferric sulfate leaching of chalcopyrite has the following overall reaction stoichiometry:

$$CuFeS_2 + 4Fe^{+3} \overset{Ag^+}{\rightleftharpoons} Cu^{+2} + 5Fe^{+2} + 2S^0$$

Two intermediate reactions in this catalytic reaction have been identified: first, an *exchange reaction* in which an argentite reaction product is deposited at the chalcopyrite surface;

$$CuFeS_2 + 4Ag^+ \rightleftharpoons 2Ag_2S_{(Surface\ CuFeS_2)} + Cu^{+2} + Fe^{+2}$$

second, an *intermediate electrochemical reaction* of Fe^{+3} with the Ag_2S film producing elemental sulfur;

$$Ag_2S_{(Surface\ CuFeS_2)} + 2Fe^{+3} \rightleftharpoons 2Ag^+ + 2Fe^{++} + S^0$$

The initial kinetics of the *exchange reaction* appear to be limited by transport through the mass transfer boundary layer as substantiated by the reaction order (1st order with respect to silver, the magnitude of the reaction velocity constant ($\sim 2 \times 10^{-2}$ cm/sec), and the temperature dependence (activation energy less than 5 kal/mole).

However, the overall leaching rate appears to be controlled by the *intermediate electrochemical reaction* of Fe^{+3} with Ag_2S crystallites as evidenced by the fact that:

1. The rate of reaction has been shown to be dependent on Fe^{+3}, Fe^{+2} and Ag^+ concentrations, but independent of the Cu^{++} concentration.
2. The apparent reaction order with respect to the Fe^{+3} concentration)0.3 M to 1.0 M Fe^{+3} for initial kinetics was estimated to be one half.
3. The rate has been found to be independent of the initial chalcopyrite particle size apparently because the reaction occurs at the surface of the Ag_2S crystallites in the argentite surface film rather than at the surface of the particles.

4. An activation energy of 15.7 kcal/mole was calculated for the initial stage of the leaching reaction (up to 50% reacted), an activation energy consistent for rate control by an electrochemical reaction.

Unlike the uncatalysed ferric sulfate leach in which elemental sulfur forms a tight, tenacious, coherent film resistant to transport, the silver catalysed ferric sulfate leach results in a porous, non-protective sulfur film due to sulfur growth on Ag_2S crystallites. It seems that only after extensive reaction (≥50%) does sufficicent sulfur form to result in a significant resistance to the rate of reaction. The increased anodic rest potentials measured for the Ag_2S coated chalcopyrite electrode suggest a shift in the polarization curve such that the reaction would be driven by a larger mixed potential. Such a phenomenon may account for the porous sulfur reaction product as has been observed to form in the leaching of chalcopyrite with stronger oxidants.

ACKNOWLEDGEMENTS

The authors wish to acknowledge the LASPAU fellowship awarded to Mr. Portillo for his studies at the University of Utah as well as financial assistance from the University of Utah Research Committee for the purchase of supplies and equipment.

REFERENCES

1. Lowe, D.F., "The Kinetics of the Dissolution Reaction of Copper and Copper-Iron Sulfide Minerals Using Ferric Sulphate Solutions," Ph.D. thesis, University of Arizona, Tucson, Arizona, 1970.

2. Linge, H.G., "A Study of Chalcopyrite Dissolution in Acid Ferric Nitrate by Potentiometric Titration," Hydrometallurgy 2, 1976, p. 51-64. See also, Ling, H.G., "Reactivity Comparison of Australian Chalcopyrite Concentrates in Acidified Ferric Solution," Hydrometallurgy 2, 1976, p. 219-233.

3. Dutrizac, J.E. et. al., "The Kinetics of Dissolution of Synthetic Chalcopyrite in Aqueous Acid Ferric Sulfate Solutions," Metallurgical Transactions, 245, 1969, p. 955-959.

4. Beckstead, L.W., et. al., "Acid Ferric Sulfate Leaching of Attritor-Ground Chalcopyrite Concentrates," Extractive Metallurgy of Copper, Vol. 2, The Metallurgical Society of A.I.M.E., New York, 1976, p. 611-632.

5. Munoz, P.B., Miller, J.D. and Wadsworth, M.E., "Reaction Mechanism for the Acid Ferric Sulfate Leaching of Chalcopyrite," Metallurgical Transactions B, 10B, June 1979, p. 149-158.

6. Sullivan, J.D., "Chemical and Physical Features of Copper Leaching," Trans. AIME, 106, 1933, p.515-546.

7. Jones, D.L. and Peters, E., "The Leaching of Chalcopyrite with Ferric Sulfate and Ferric Chloride," Extractive Metallurgy of Copper, Vol. 2, The Metallurgical Society of A.I.M.E., New York, 1976, p.633-653.

8. Baur, J.P., Gibbs, H.L. and Wadsworth, M.E., "Initial-Stage Sulfuric Acid Leaching Kinetics of Chalcopyrite Using Radiochemical Techniques," U.S.B.M., R.I. 7823, 1974.

9. Peters, E., "The Physical Chemisty of Hydrometallurgy," Internat. Symp. on Hydromet. AIME New York, 1973, p. 205-228.

10. Warren, G. and Wadsworth, M.E., "Hydrometallurgy of Fine Mineral Particles," International Symposium of Fine Mineral Particles, A.I.M.E., Las Vegas, Nevada, Feb. 1979.

11. Pawlek, F.E., "The Influence of Grain Size and Mineralogical Composition on the Leachability of Copper Concentrates," Extractive Metallurgy of Copper, Editors Yannopoulos and Agarwal, A.I.M.E. 1976.

12. McElroy, R.O. and Duncan. D.W., British Columbia Research Council, Vancouver, Canada V6F 212, The Silver Institute Letter, 5, No. 8, Sept. 1975.

13. Snell, G.J. and Sze, M.C., "New Oxidative Leaching Process Uses Silver to Enhance Copper Recovery," EMJ, 178, No. 10, October 1977, p. 100-105.

14. Miller, J.D. and Portillo, H.W., "Silver Catalysis in Ferric Sulfate Leaching of Chalcopyrite," XIII International Mineral Processing Congress, Warsaw, Poland, 1979, p. 691-742.

15. Portillo, H.W., "Silver Catalysis in the Acid Ferric Sulfate Leaching of Chalcopyrite," M.S. Thesis, Dept. Metallurgy and Metallurgical Engineering, University of Utah, Salt Lake City, Utah 1978.

16. Wadsworth, M.E. and Miller, J.D., "Hydrometallurgical Processes." Rate Processes of Extractive Metallurgy, Plenum Press, 1978, p. 222.

17. Ranz, W.E.,and Marshall, W.R., Chem Eng. Progr., 48, 1952, p. 141.

18. Vesely, J., Jensen, O.J., and Nicolaisen, B., "Ion-Selective Electrodes Based on Silver Sulfide," Analytica Chimica Acta, 62, 1972, p. 1-13.

19. Helgeson, H.C., "Thermodynamics of Hydrothermal Systems at Elevated Temperatures and Pressures," American Journal of Science, 267, Summer 1969, p. 729-834.

20. Robie, R.A. and Waldbaum, D.R., "Thermodynamic Properties of Minerals and Related Substances at 25°C and One Atmosphere Pressure and at Higher Temperatures," Geological Survey Bulletin 1269.

21. Vetter, K.J., Electrochemical Kinetics Theoretical and Experimental Aspects, Academic Press, N.Y., 1967.